Journal of Hydrology 597 (2021) 126155

Contents lists available at ScienceDirect

Journal of Hydrology

journal homepage: www.elsevier.com/locate/jhydrol

Research papers

Change of rainfall–runoff processes in urban areas due to high-rise buildings

Chulsang Yoo, Eunsaem Cho *, Wooyoung Na, Minseok Kang, Munseok Lee

School of Civil, Environmental and Architectural Engineering, College of Engineering, Korea University, Seoul 02841, South Korea

ARTICLE INFO

This manuscript was handled by Marco Borga, Editor-in-Chief, with the assistance of Michael Bruen, Associate Editor

Keywords:
High-rise building
Rainfall-runoff analysis
Rainfall-runoff experiment
Shot noise process model

ABSTRACT

This study proposes a method to consider the high-rise building in the rainfall–runoff analysis of an urban basin. This study uses a rainfall–runoff model based on the shot noise process to evaluate the relative roles of the building rooftop sub-basin and the wall sub-basin. In addition, the rainfall–runoff experiment is conducted in a laboratory environment to validate the proposed method considering high-rise buildings. The major results of this study can be summarized as follow. (1) The rainfall intercepted by the building wall increases the runoff volume and peak flow, but the longer flow path from the rooftop basin decreases the peak flow. Overall, the role of the building wall is found to be more significant than the rooftop in resulting in increased runoff volume and peak flow. (2) The experimental results also confirm the simulation results. The contribution of the building wall to the peak flow is found to be highly significant, especially when the wind speed is high. For example, when the mean wind speed is 1.11 m/s, the contribution of the building wall to the peak flow is found to be 6.3 – 6.9% and 14.2 – 17.0% for the 1.0 and 1.4 m building height, respectively. (3) The accuracy of the rainfall-runoff model can be improved by considering the building. As the building is considered, the RMSE and the difference of peak flow between the observed and simulated hydrograph decrease in all cases. The results of this study support the idea that, in the urban basin, the contribution of the high-rise building to runoff can be significant.

1. Introduction

Urbanization is a common issue worldwide. More than 50% of the world population lives in cities (Seto and Shepherd, 2009; Douglas, 2012; Zhou et al., 2015; Phillis et al., 2017; Cleophas et al., 2019). During the 20-year period 1990 – 2010, the urban area increased by more than 70% (Zhou et al., 2015; Liu et al., 2018). The number of megacities with population of 10 million or greater is also expected to rise from 33 to 43 in the period 2018 to 2030 (DESA, 2018). In those cities, the numbers of so-called high-rise buildings (e.g., 300-meter-or-higher tall buildings) are also increasing (Safarik et al., 2015; Gabel and Shehadi, 2017). Increased impervious area in the city increases the runoff volume, as well as the runoff peak. The peak time has also been shortening to increase flood risk (Liu et al., 2005; Nirupama and Simonovic, 2007; Saghafian et al., 2008; Suriya and Mudgal, 2012). More and more city residents are threatened by the increased flood risk (Cançado et al., 2008; Tingsanchali, 2012).

The effect of urbanization on the rainfall–runoff analysis has been one of the most important issues in hydrology (Hejazi and Markus, 2009; Roy et al., 2009; O'Driscoll et al., 2010; Du et al., 2012; Li et al., 2013; Chen et al., 2015; Prosdocimi et al., 2015; Yao et al., 2016; Jung and Kim, 2017; Niemi et al., 2019). Most of these studies have focused on urban flood, although some studies have also raised the problems of decreased infiltration and dry stream (Roy et al., 2009; O'Driscoll et al., 2010; Jung and Kim, 2017). In those analyses, urbanization is considered simply by increasing the impervious area. That is, the impervious area is the sole and key factor used to consider urbanization. Models like ILLUDAS (Terstriep and Stall, 1974), SWMM (Cole and Shutt, 1976), TR-55 (USDA, 1985), HSPF (Bicknell et al., 1996), and STORM (Wiles and Levine, 2002) have been used for this purpose.

However, recent megacities are characterized by the high-rise building. These cities are totally different from conventional cities that are simply characterized by the urban area or impervious area. Megacities are three-dimensional in reality. While the conventional two-dimensional cities are characterized by impervious area, megacities should be characterized by additionally considering the high-rise building. That is, the conventional two-dimensional cities consider the change of infiltration to be important, but the three-dimensional

* Corresponding author.
E-mail addresses: envchul@korea.ac.kr (C. Yoo), saemrnt@gmail.com (E. Cho), uoo921227@gmail.com (W. Na), minseok0517@hanmail.net (M. Kang), ans918@korea.ac.kr (M. Lee).

https://doi.org/10.1016/j.jhydrol.2021.126155
Received 2 September 2020; Received in revised form 26 February 2021; Accepted 1 March 2021
Available online 5 March 2021

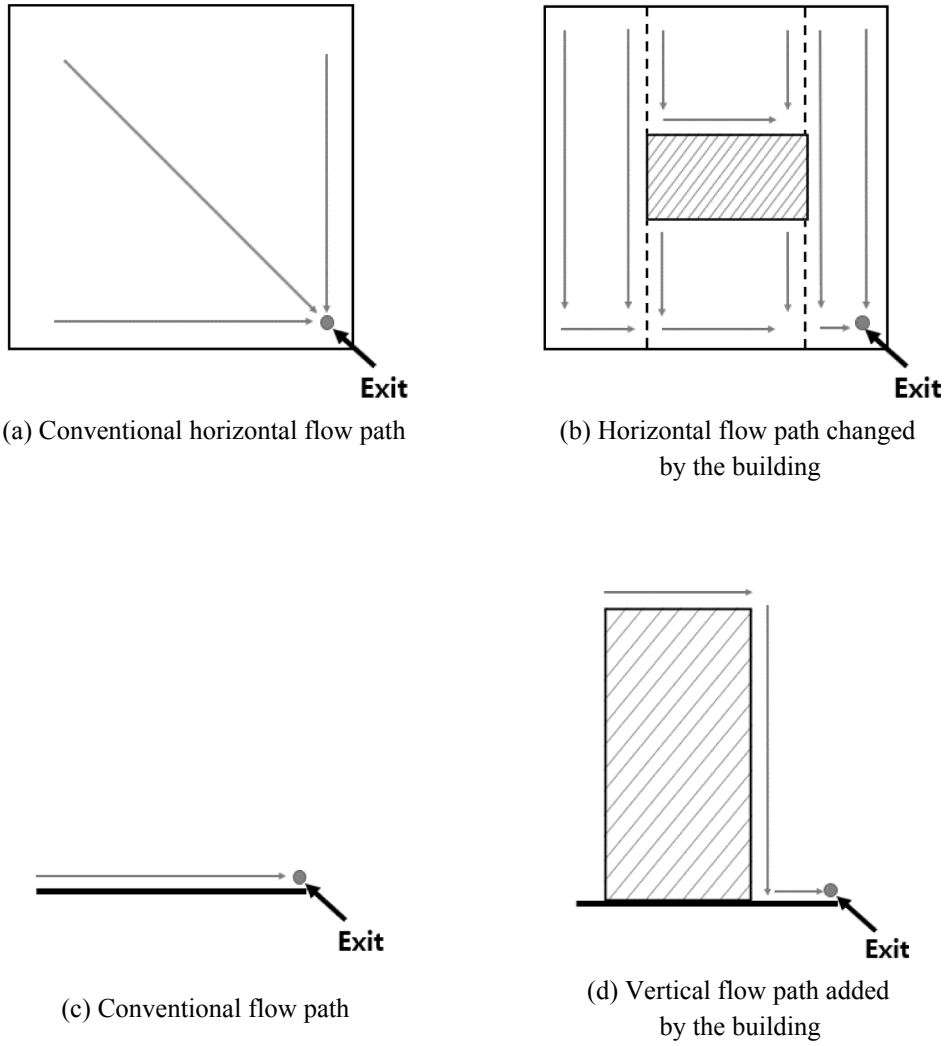

(a) Conventional horizontal flow path

(b) Horizontal flow path changed by the building

(c) Conventional flow path

(d) Vertical flow path added by the building

Fig. 1. Comparison of conventional flow path and changed flow path by a building.

megacities should additionally consider the rainfall interception by the high-rise building. In previous studies, the interception on buildings was considered as a loss (Grimmond and Oke, 1991; Lemonsu et al., 2007; Hamdi et al., 2011), or buildings were regarded as a factor that slows the runoff (Schubert et al., 2008; Cea et al., 2010; Chan, 2012; Dottori and Todini, 2013). However, in the three-dimensional city, the intercepted rainfall should be analyzed as an additional source of runoff.

The role of interception by the high-rise building in an urban basin is similar to the role of high mountains in a natural basin. Both high-rise buildings and high mountains have a major effect on the interception of rainfall that falls obliquely due to the wind. It is difficult to find previous studies on the phenomenon that rainfall-runoff characteristics are changed by high-rise buildings. On the other hand, the authors could find several references of analyzing the effect of the high mountains. For example, Hughes et al. (2009) showed the role of the mountain (specifically, Big Pine Mountain, located in California) is to make different runoff patterns on its coastal side and its inland side. Simply, the mountain intercepts rainfall to make additional runoff on the coastal side. A similar result can also be found in Murphy et al. (2017), who compared the runoff on the eastern and western sides of Luquillo Mountain in Puerto Rico. The total amount of rainfall on the western side of Luquillo Mountain was found to be 46% higher than that on the eastern side. The role of the high-rise buildings in megacities can be assumed to be similar to those mountains.

It should also be mentioned that the high-rise building changes and complicates the route of runoff. The change is also dependent upon the shape of the building, as well as the density of buildings in an urban area. The raindrops that have reached the wall of a building roll down for a while, and then free fall again to the ground. The rainfall on the rooftop of a building is generally drained through the vertical pipe.

Various studies have been done for the runoff on the wall of a building (Beijer and Johansson, 1977; Hall and Kalimeris, 1982; Blocken and Carmeliet, 2012). For example, Beijer and Johansson (1977) simulated the runoff on the wall of a building using a simple rainfall–runoff model. Hall and Kalimeris (1982) calculated the runoff depth on the wall, which was then used to estimate the flow velocity. Blocken and Carmeliet (2012) numerically simulated the runoff on the wall to show that the flow itself is very similar to that in the open channel. These studies confirm that the runoff does exist on the wall of a building, which can also be considered in the rainfall–runoff analysis in an urban basin.

The objective of this study is to consider the high-rise buildings in the rainfall–runoff analysis of an urban basin. In particular, the difference should be evaluated between the conventional two-dimensional rainfall–runoff analysis and the three-dimensional analysis considering the high-rise building. The rainfall–runoff analysis method in this study is basically simulation-based, and some additional experiments will also be conducted in a laboratory environment to validate the proposed method.

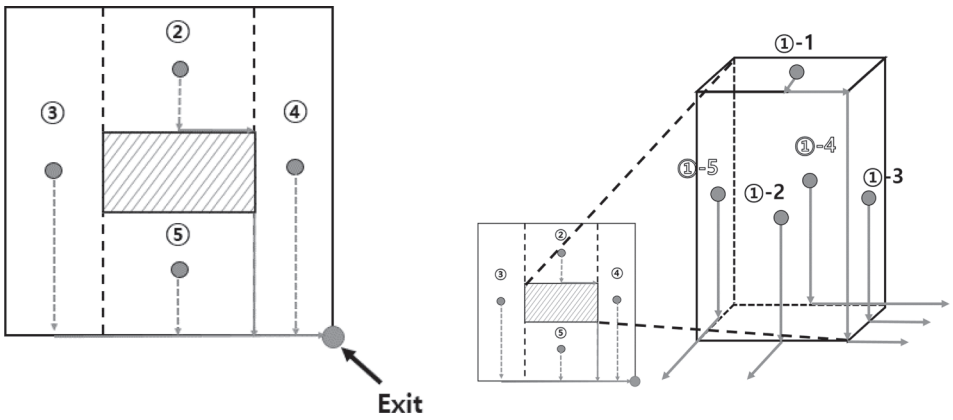

(a) Sub-basin division and flow path in typical urban basin

(b) Sub-basin division and flow path in urban basin with the high-rise building

Fig. 2. Comparison of sub-basin division and flow path in urban basin with and without the high-rise building.

2. Distortion of the rainfall–runoff process by high-rise buildings

2.1. Rainfall interception

In general, the amount of intercepted rainfall is regarded as being evaporated and does not contribute to the runoff during the short-term of the rainfall–runoff process. On the other hand, rainfall intercepted by a high-rise building could reach the ground and contribute to the runoff. Therefore, the intercepted rainfall, in this case, may not be assumed to be evaporated as in the conventional rainfall–runoff analysis method.

Cho et al. (2020) proposed an empirical equation for estimating the amount of rainfall intercepted by a building wall. The basic form of the empirical equation was determined by analyzing prior studies on the spatial distribution of wind-driven rain (WDR), and a laboratory experiment was conducted to fit the proposed empirical equation. In addition, the empirical equation was validated by comparing its estimates with the in-situ observation. The empirical equation proposed by Cho et al. (2020) is as follows:

$$Q = 0.161 \times B \times H \times U \times R_h^{0.88} \quad (1)$$

where R_h is the rainfall intensity observed at the ground (mm/h), B is the width of the building wall (m), H is the height of the building wall (m), U is the wind speed (m/s), and Q is the amount of intercepted rainfall ($m^2 \cdot$mm/h). In this study, the amount of intercepted rainfall was estimated using Eq. (1), which was then used as input data for the runoff analysis from the wall of a high-rise building.

2.2. Three-dimensional flow path

Consideration of the high-rise building changes the flow path of runoff in the basin. Generally, the flow path is considered over the two-dimensional plane. The flow length is estimated as the horizontal distance, and the flow velocity is determined by considering the slope of the land surface. In urban basins, buildings are assumed to be simply a part of the impervious area. The building's shape including the height and width, is not considered in the flow path. In some two-dimensional rainfall–runoff models, the flow path on the land surface is determined by considering the barrier role of a building (Seyoum et al., 2012; Bisht et al., 2016; Leandro and Martins, 2016; Huang and Jin, 2019).

Fig. 1 shows the possible change of flow path due to high-rise building. Fig. 1(b) shows the changed flow paths due to a high-rise building over the two-dimensional plane, which are very different from the conventional one, as shown in Fig. 1(a). Additionally, the high-rise building makes the flow path three-dimensional (Fig. 1(d)). The flow path cannot be two-dimensional, such as in the conventional model (Fig. 1(c)). The vertical path is especially important in the case that the travel time from the rooftop of a building to the ground is relatively long. In a small urban center with many high-rise buildings, this change will surely be concentrated. In this case, the flow path from the building wall to the ground can also be important.

2.3. Sub-Basin division

The sub-basin division is important to consider various areas with different characteristics in the runoff estimation. In particular, the high-rise building itself can be divided into several sub-basins. Fig. 2(b) shows an example of the sub-basin division of a high-rise building. The conventional method of sub-basin division is as in Fig. 2(a), even in the case of considering a building as a barrier against surface runoff.

Fig. 2(b) shows that the high-rise building can be divided into one sub-basin of the rooftop and four building walls. The flow path from the rooftop of a building (sub-basin ①-1) includes the rooftop itself, and the flow through the vertical drainage pipe. The flow path from the building wall (sub-basins ①-2 – ①-5) is composed of the surface flow on the building wall, and the free fall again to the ground. In particular, when the wind is rather high, the sub-basins ①-2 – ①-5 (i.e., building walls) are important. If the wind speed is greater than 8.2 m/s, the intensity of wind-driven rain on building walls can be higher than that on the rooftop of a building (Cho et al., 2020). In this case, the slope of wind-driven rain becomes 45°, determined by comparing the terminal velocity of a raindrop and the wind speed.

3. Rainfall–runoff model and parameters

3.1. Model

This study uses the rainfall–runoff model proposed by Kang and Yoo (2018). This rainfall–runoff model is based on the concept of the shot noise process (Weiss, 1977). The shot noise process was developed to model the noise from a diode or transistor. This noise has the peak at the occurrence point, and as time continues, decays exponentially. Due to the characteristic feature of the noise, it is called as a shot noise. If many noises occur, the resulting overall noise simply becomes the sum of each noise.

Kang and Yoo (2018) proposed the use of the shot noise process to model flood runoff. In fact, the shot noise process model has been used more to model the long-term runoff, rather than the flood. This is because the sharp peak at the occurrence of the noise was assumed to be inappropriate to model flood runoff. However, the concept of the linear

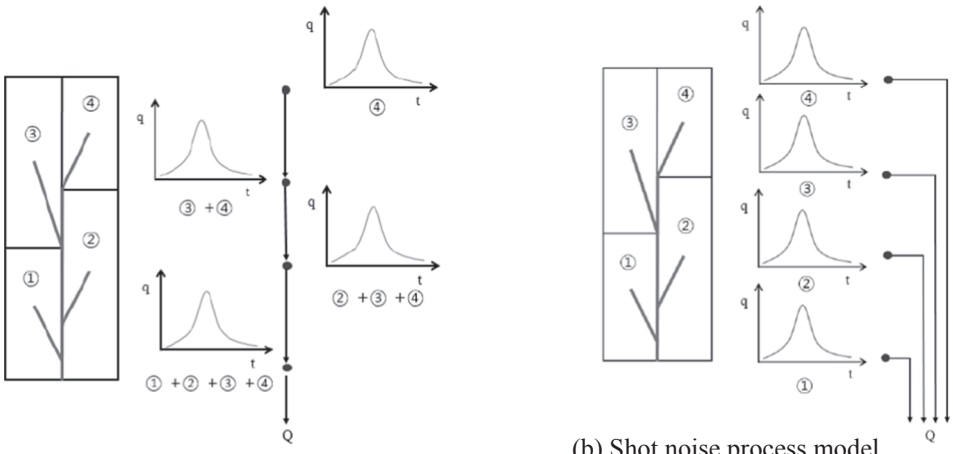

(a) Conventional rainfall-runoff model

(b) Shot noise process model (Kang and Yoo, 2018)

Fig. 3. Comparison of the concept of shot noise process model with that of conventional rainfall-runoff model.

reservoir model, which also produces a shot-noise-like response function, has been frequently used in the modeling of the instantaneous unit hydrograph (Nash and HRS, 1960; Diskin et al., 1973; Singh, 2004; Sahoo et al., 2006). As many shot noises or linear reservoirs are considered, the characteristic feature of each shot noise naturally disappears.

Another interesting feature of the shot noise process considered by Kang and Yoo (2018) is that the sum of each shot noise simply becomes the overall result. That is, different from other rainfall-runoff models, channel flood routing is not considered. The runoff from any sub-basin is considered as a single shot noise. The shape of the shot noise can be different according to the sub-basin characteristics, channel characteristics to the exit of the basin, and the rainfall input. However, each shot noise becomes independent from others as all of them flow to the exit of the basin. Each shot noise is simply added at the exit of the basin (see Fig. 3). As this study assumes that the rooftop of a building, as well as each building wall, is an independent sub-basin, it is easy to evaluate the contribution of each sub-basin to the total runoff at the exit of the basin.

The runoff at the exit of the basin due to a unit effective rainfall can be expressed as a sum of shot noises from all contributing sub-basins.

$$U(t) = \sum_n P_n e^{-\frac{(t-t_{c(n)})}{K_n}} \tag{2}$$

where, n is the number of sub-basins, P_n is the peak value of the runoff generated by the unit effective rainfall from each sub-basin, $t_{c(n)}$ is the travel time from the center of each sub-basin to the exit of the basin, and K_n is the decay coefficient of the shot noise or the storage coefficient representing the entire flow path from the center of the sub-basin to the exit of the basin. In this study, as the basin area is small, the rainfall intensity is assumed to be the same all over the basin. As a result, the runoff hydrograph due to continuous rainfall can be derived as follows:

$$O(t) = \sum_i R_i \times U(t-i) = \sum_i R_i \left[\sum_n P_n e^{-\frac{(t-i)-t_{c(n)}}{K_n}} \right] \tag{3}$$

where, i represents the time of rainfall occurrence, and R_i represents the rainfall intensity.

The parameters of the rainfall–runoff model are the peak value (P_n), the travel time ($t_{c(n)}$) and the decay coefficient (K_n) of the shot noise representing each sub-basin. First, the travel time ($t_{c(n)}$) is determined as the sum of each travel time from the center of the basin to the exit of the basin. The surface runoff of the sub-basin and several open channel flows are considered to estimate the travel time. In ungauged basins, empirical equations are generally used to estimate the travel time. The Kirpich (Kirpich, 1940), Rziha (Rziha, 1876), Kraven (I) (JSCE, 1999), Kraven (II) (JSCE, 1999), and Kerby (Kerby, 1959) formulae are among those that are available for this purpose. Each formula was derived under certain specific conditions, which should also be considered in its application. If the observed data are available, the travel time can be easily estimated.

The decay coefficient (K_n) can be replaced by the storage coefficient. This arises from the fact that the shot noise process is also the response of a linear reservoir. Basically, the storage coefficient can be estimated by analyzing the observed data. However, in the case of ungauged basins, the storage coefficient should also be estimated using some empirical equations. The equations of Clark (1945), Linsley (1945), Russell et al. (1979) and Sabol (1988) are among those frequently used.

Finally, the peak value (P_n) is determined by considering the total runoff volume at each sub-basin. The total runoff volume (*Volume*) at each sub-basin can be easily estimated by applying the modified rational formula with the given runoff coefficient (Hua et al., 2003):

$$Volume = P_n \int_0^\infty e^{-\frac{t}{K_n}} dt \tag{4}$$

3.2. Travel time and storage coefficient

In a small urban basin, the travel time of a raindrop, even from the farthest point, is not long. It can take just a few minutes to reach the nearest manhole. However, if considering a high-rise building, the flow path can be longer, and thus the travel time can also be longer. Obviously, a longer travel time alleviates peak flow, but the problem is that the high-rise building has four walls and a rooftop to contribute to runoff. How to consider these changes is of interest in this study.

Estimation of the travel time is thus important in this study. First, the rainfall on the rooftop of a building reaches the ground via three different paths: One is the flow on the rooftop to the inlet of the vertical drainage pipe, next is the flow in the vertical drainage pipe, and finally, there is the flow on the ground from the exit of the vertical drainage pipe to the nearest manhole. The travel time in the first and third paths may be estimated by the Kraven (II) formula or the Kerby formula. In particular, the Kerby formula is applied to a very small basin of less than 0.04 km^2, so it is useful to estimate the travel time in a lab experiment (Soliman, 2010). The Kraven (II) formula is also known to be valid for small basins. The Kerby and Kraven (II) formulae are as follow:

$$t_c = 36.264 \frac{(Ln)^{0.467}}{S^{0.2335}} \tag{5}$$

$$t_c = 16.667\frac{L}{V} \quad (6)$$

where t_c is the travel time (min), L is the flow length (km), n is the roughness coefficient, S is the slope of the basin, and V is the flow velocity (m/s). In Eq. (6), for the slope less than 0.005, the flow velocity $V = 2.1$ m/s is applied; and for the slope higher than 0.005, but less than 0.01, $V = 3.0$ m/s is applied. For the slope higher than 0.01, $V = 3.5$ m/s is applied.

The travel time in a vertical drainage pipe can be estimated by Wyly and Eaton formula (Wyly and Eaton, 1961). Their formula provides the mean falling velocity:

$$v_{pipe} = 16.2\left(\frac{Q}{d}\right)^{0.4} \quad (7)$$

where v_{pipe} is the fall velocity (m/s) in a vertical drainage pipe, Q is the flow rate (m^3/s), and d is the diameter (m) of the pipe. The flow rate is generally estimated by applying the rational formula (Ponce, 1989; Maidment, 1993; Bedient et al., 2008), and the diameter of the pipe is assumed to be 0.2 m, which is the maximum one available for the high-rise building (ME, 2015).

The travel time of a raindrop rolling down the building wall was estimated using the experimental result by De Vogelaere and Pacco (2012). According to their study, the mean velocity of a raindrop rolling on a similar wall to that in this experiment is 0.027 m/s. In fact, this velocity is very slow to make the travel time so long in a tall building. Thus, one more assumption should be introduced for application on the real urban basin, which is that the raindrop becomes larger as it rolls down the wall, and finally becomes detached from the wall to free fall.

The free-fall velocity can be estimated by the equation proposed by Ferro (2001):

$$v_{free} = v_{max}(1 - e^{-a_n \times d}) \quad (8)$$

where v_{free} represents the mean free-fall velocity (m/s), v_{max} is the maximum free-fall velocity (m/s), d is the diameter of a raindrop (mm), and a_n is a parameter determined by considering the experimental conditions. When the drop height of a raindrop is higher than 20 m, then v_{max} and a_n are assumed to be 9.55 m/s and 6, respectively. The diameter of a raindrop used in this study was the median value representing the given rainfall intensity (Rziha, 1876).

The storage coefficient is more complicated to determine. This is affected by the basin characteristics, as well as the channel characteristics. If some amount of rainfall–runoff data are available, it may be estimated. In ungauged basins, any given empirical formula, if it is available, must be relied on. However, it may be an exceptional situation for a reliable formula to be given. On the other hand, in this study, the authors relied on the study of Russell et al. (1979), where the storage coefficient was assumed to be more or less the same as the concentration time (i.e., the overall travel time to the exit of the basin for each sub-basin). Kang and Yoo (2018) also assumed the storage coefficient to be identical to the concentration time. This assumption may not be strictly accurate but may be acceptable in the study of handling the rainfall–runoff analysis in an urban basin.

4. Validation of rainfall–runoff analysis in the experimental basin

4.1. Experimental setting

In general, laboratory experiment had been conducted to analyze factors affecting rainfall-runoff processes (Pappas et al., 2008; Shuster et al., 2008; Shuster and Pappas, 2011; Isidoro et al., 2012; Isidoro and De Lima, 2014; Leandro et al., 2016; Ferreira et al., 2019; Liu et al., 2020). This study prepared an experimental basin with the rainfall nozzles and fans for the rainfall–runoff experiment. The experimental basin was slanted by 10°, and a basin outlet was located in the lower right corner. Fig. 4(a) shows a schematic diagram of the experimental basin. 10 nozzles (diameter 0.5 mm) were used to simulate rainfall, and 12 fans to simulate wind. There are two rows of five rain nozzles, and the height of each row is 2.61 m and 2.71 m from the experimental basin. Simply, the average height of all rainfall nozzles is 2.66 m. In the case of

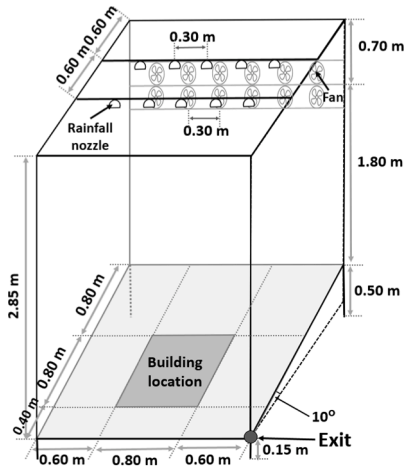

(a) without the building model

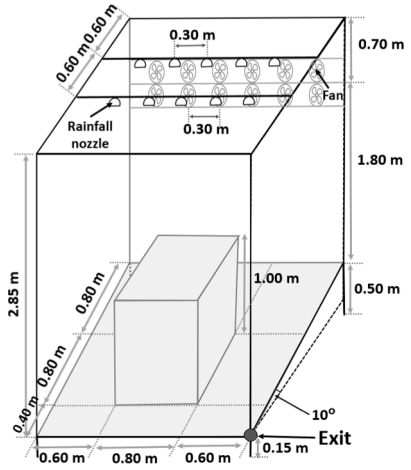

(b) with the building model (height = 1.0 m)

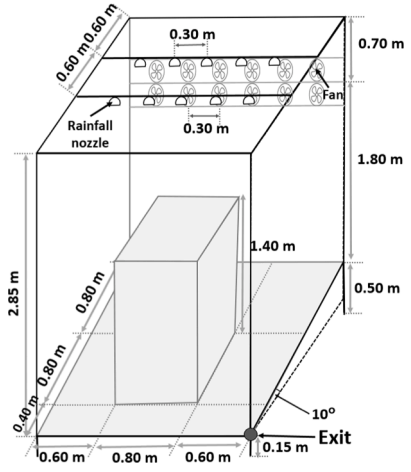

(c) with the building model (height = 1.4 m)

Fig. 4. Schematic diagram of experimental basin for rainfall-runoff experiment.

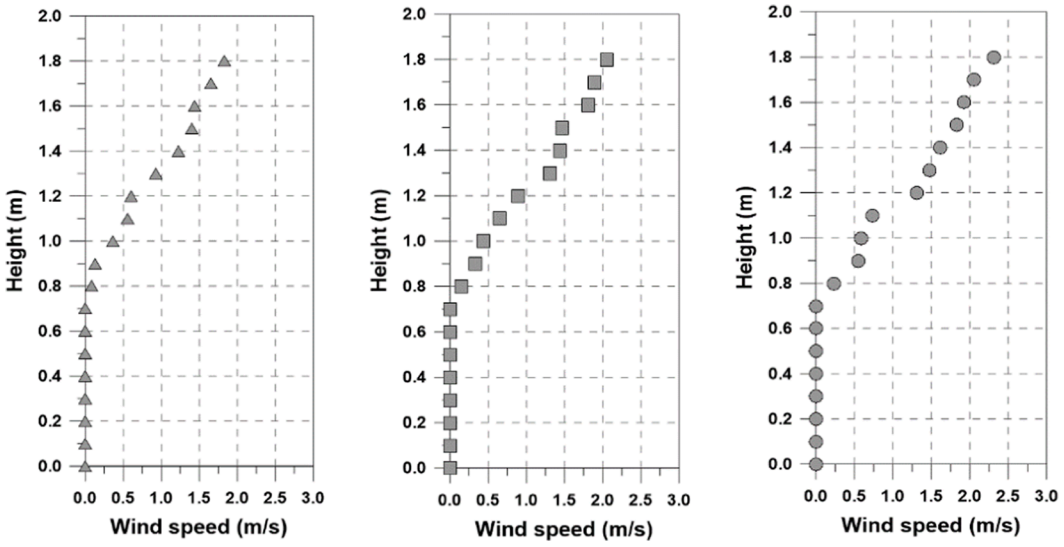

Fig. 5. Average wind speed by height over input voltage.

Table 1
Wind speed at the height of the building model.

Voltage (V)	Height (m)	Wind speed (m/s)
140	1.00	0.36
	1.40	1.23
180	1.00	0.44
	1.40	1.44
220	1.00	0.59
	1.40	1.62

12 fans, the average height is 1.80 m from the experimental basin. In Fig. 4(a), the building location indicates where the building model will be placed.

The width and length of the building were fixed in this experiment as 0.8 m, but two different heights of the building, 1.0 and 1.4 m, were considered. In addition, the rainfall–runoff experiment without any building was also conducted to evaluate the effect of the building. Fig. 4 (b) and 4(c) show schematic diagrams of building models with their heights 1.0 and 1.4 m, respectively.

In this experiment, the wind speed was controlled by adjusting the voltage of the power supply of the fan. Three different voltages, i.e., 140, 180, and 220 V, were used for the fan. The location of the wind speed measurement was done at the cross-section 1.2 m apart in front of the fan. The cross-section was then divided into six columns, and, for each column the wind speed measurement was done at every 0.1 m interval from the bottom to the top 1.8 m. The measurement was repeated several times to obtain the valid value. Fig. 5 shows the vertical variation of the wind speed with respect to the input voltage.

Obviously, the distributions of the average wind speed are different depending on the input voltage. The average wind speed was up to 1.83 m/s at 140 V, 2.05 m/s at 180 V, and 2.31 m/s at 220 V. Table 1 summarizes the wind speed at the building height for each input voltage. The cross-sectional average of the wind speed for each voltage was then calculated to be 0.80 m/s for 140 V, 0.94 m/s for 180 V, and 1.11 m/s for 220 V. These cross-sectional averages were similar regardless of the building height.

The rainfall intensity was controlled by changing the flow rate of the pump. Three flow rates, i.e., 2.0, 2.5, and 3.0 L/min, were considered in this experiment. The rainfall intensity on the experimental basin was not evenly distributed, so the representative rainfall intensity was determined as the mean of nine measurements over the experimental basin.

Table 2
Representative rainfall intensity based on wind speed and pump flow rate condition.

Pump flow rate (L/min)	Wind speed (m/s)	Rainfall intensity (mm/hr)
2.0	0.80	27.3
	0.94	25.9
	1.11	21.4
2.5	0.80	32.5
	0.94	29.3
	1.11	24.6
3.0	0.80	37.7
	0.94	33.2
	1.11	27.2

That is, the experimental basin was divided into nine equal zones, and the rainfall intensity was measured at the center of each zone. The representative rainfall intensity was then determined to be their arithmetic average. The measurements were repeated three times, and finally, their average was used as the rainfall condition in this study.

The authors found that the rainfall measurement method in this study was very similar to that of Isidoro et al. (2012). Isidoro et al. (2012) measured the rainfall intensity at every 0.3 m intervals over the 2 m × 2 m experimental basin. Also, Isidoro et al. (2012)) repeated measurement three times to determine the rainfall condition.

Table 2 summarizes the representative rainfall intensities determined with respect to various conditions. Table 2 shows that as the pump flow rate increases, the rainfall intensity increases. On the other hand, as the wind speed increases, the rainfall intensity decreases. Obviously, as the wind speed increases, a significant amount of raindrops fall outside of the experimental basin. This is the reason why as the wind speed increases, the rainfall intensity decreases. When the pump flow rate was the highest (i.e., 3.0 L/min) and the wind speed was the lowest (i.e., 0.8 m/s), the average rainfall intensity was the highest at 37.7 mm/h. In contrast, when the pump flow rate was the lowest (i.e., 2.0 L/min) and the wind speed was the highest (i.e., 1.11 m/s), the average rainfall intensity was the lowest at 21.4 mm/h.

The rainfall-runoff experiment using several buildings had been conducted in previous studies (Isidoro et al., 2012; Liu et al., 2020). On the other hand, in this study, only one building is considered, and experiments are conducted by changing the height of the building with various rainfall and wind speed conditions. Through these experiments, this study evaluates the effect of the intercepted rainfall by a building

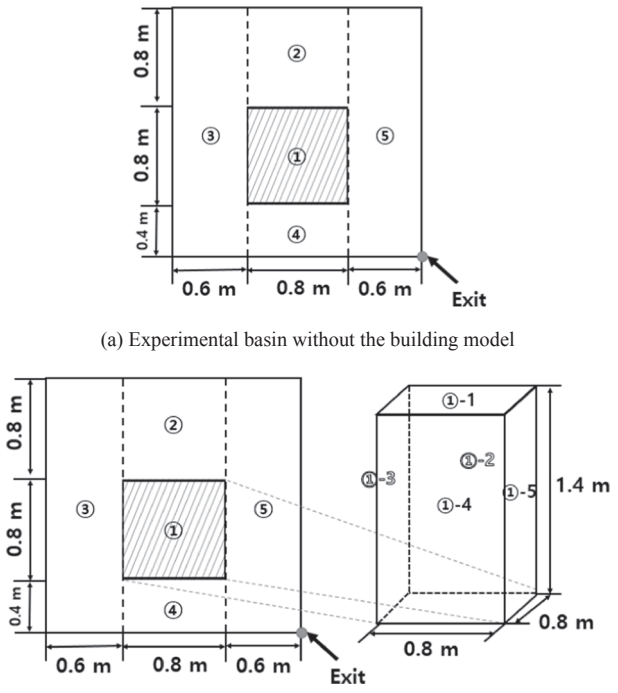

(a) Experimental basin without the building model

(b) Experimental basin with the building model

Fig. 6. Sub-basin division of experimental basin with and without the building.

model on the rainfall-runoff process under various rainfall, wind speed conditions. In addition, the authors try to show that the influence of the building, which would be verified by the experiment, can be theoretically simulated by the rainfall-runoff model.

4.2. Rainfall–runoff analysis

4.2.1. Sub-basin division and travel time

Fig. 6 shows that the sub-basin division was done by considering the rooftop and each wall of the building located at the center of the basin. To compare the runoff results from the basin with and without the building, the basin without the building was also divided into five sub-basins (Fig. 6(a)). With the building at the center of the basin, the total number of sub-basins was increased to be eight (Fig. 6(b)). In this case, the rooftop of the building (sub-basin ①-1) has a longer travel time than the sub-basin ①, as the raindrops on the rooftop should drain by rolling down the building wall. Also, in this experiment, not all four building walls contribute to the runoff. Depending on the wind direction, just one or two walls contribute to the runoff. This is also the same in the real world. In this experiment, just one building wall, the sub-basin ①-2 was considered in the runoff estimation.

Table 3 summarizes the basic characteristics of each sub-basin (without the building). The sub-basin area varies from 0.32 to 1.20 m^2. The flow length was determined separately for the inside and outside of the sub-basin. The flow length inside of the sub-basin indicates the length from the farthest point to the exit of the sub-basin. Also, in additional to the slope 10° in the flow direction of the basin, the slopes in the cross direction were all assigned to be 0.1°. This slope in the cross direction was introduced to apply the empirical formulae to estimate the travel time.

The area and flow length of the sub-basin ①-1 are the same as those of the sub-basin ①, but the slope inside of the sub-basin ①-1 is assumed to be 0.1°. The flow length outside of the sub-basin ①-1 additionally includes the height of the building. The area of the sub-basin ①-2 varies, according to the height of the building. The flow length within the sub-basin is the same as the building height, and the flow length outside of the sub-basin becomes 1.4 m in the cross direction, and 1.2 m in the flow direction.

The formulae by Kerby (1959) and De Vogelaere and Pacco (2012) were used in this study to estimate the travel time. The formula by Kerby (1959) was used to estimate the travel time on the rooftop of the building, and that on the land surface. The roughness coefficient required to apply the Kerby formula was assumed to be 0.01 for the wood (rooftop and wall of the building), and 0.009 for the acrylic (basin surface).

The travel time on the building wall was estimated by applying the experimental result of De Vogelaere and Pacco (2012). Based on De Vogelaere and Pacco (2012), the flow velocity of a raindrop rolling down the building wall is about 0.027 m/s. The travel time in the building wall was thus estimated simply by dividing the building height by this flow velocity. In reality, the raindrops that reach the rooftop of a building are collected and drained by vertical pipes; but in this experiment, they are drained simply by rolling down the building wall.

Table 4 summarizes the travel time estimated for each sub-basin in Fig. 5(a) and 5(b). Both inside and outside the sub-basin were considered to estimate the travel time. As the slope in the cross direction was assumed to be small, the travel time was estimated longer if the travel path included a rather long portion in the cross direction.

Table 4
Travel time of sub-basins based on the height of the building.

Building height (m)	Sub-basin number	Inside travel time (sec)	Outside travel time (sec)	Total travel time (sec)
0	①	12.9	58.8	71.7
	②	12.9	65.1	78.0
	③	19.9	58.4	78.3
	④	9.4	49.4	58.8
	⑤	19.9	33.3	53.2
1.0	①-1 (rooftop)	61.3	95.8	157.1
	①-2 (wall)	37.0	65.1	102.1
	②	12.9	65.1	78.0
	③	19.9	58.4	78.3
	④	9.4	49.4	58.8
	⑤	19.9	33.3	53.2
1.4	①-1 (rooftop)	61.3	110.6	171.9
	①-2 (wall)	51.9	65.1	117.0
	②	12.9	65.1	78.0
	③	19.9	58.4	78.3
	④	9.4	49.4	58.8
	⑤	19.9	33.3	53.2

Table 3
Basic characteristics of each sub-basin without the building.

Sub-basin number	Sub-basin area (m^2)	Flow length (m)			Slope (°)		
		Inside	Outside Flow direction	Cross direction	Inside	Outside Flow direction	Cross direction
①	0.64	0.8	0.4	1.4	10.0	10.0	0.1
②	0.64	0.8	1.2	1.4	10.0	10.0	0.1
③	1.20	2.0	0.0	2.0	10.0	10.0	0.1
④	0.32	0.4	0.0	1.4	10.0	10.0	0.1
⑤	1.20	2.0	0.0	0.6	10.0	10.0	0.1

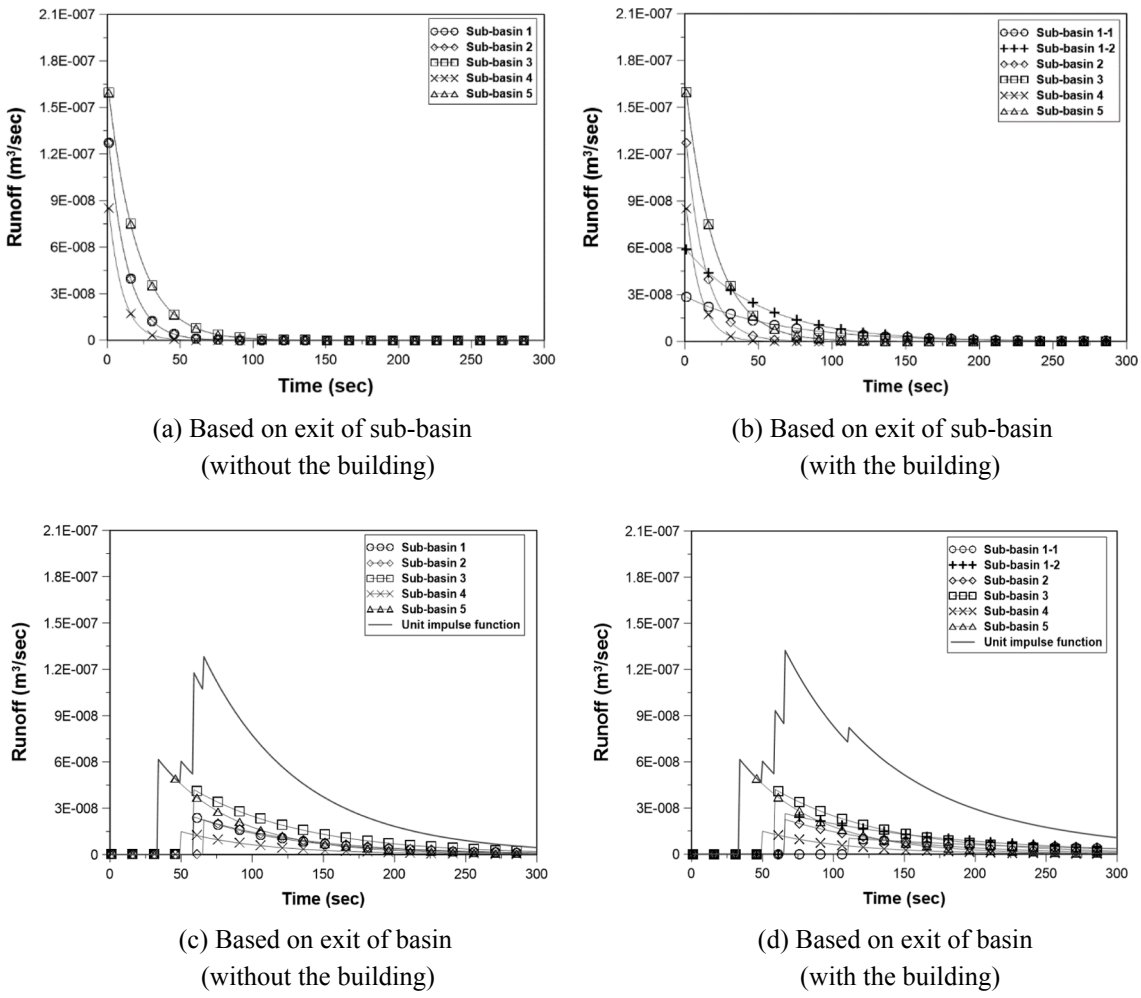

(a) Based on exit of sub-basin (without the building)

(b) Based on exit of sub-basin (with the building)

(c) Based on exit of basin (without the building)

(d) Based on exit of basin (with the building)

Fig. 7. Comparison of unit impulse function with and without the building.

As can be found in Table 4, the travel time for the sub-basins ②–⑤ remained the same in both cases of with or without the building at the center of the basin. However, the sub-basin ① in Fig. 6(a) was divided into two sub-basins ①-1 and ①-2 as a building was introduced, such as in Fig. 6(b). As the wind direction in this experiment was fixed to be perpendicular to the building wall, in this case only one building wall ①-2 was considered. The travel time of sub-basin ①-1 is very different from that of sub-basin ①. One reason is that the building wall is additionally considered in its estimation, and the second reason is that the slope of the rooftop of the building is assumed to be much milder than that of the basin surface. The decay coefficient of all the basin was assumed to be the same as its travel time. This assumption is based on Russell et al. (1979), in which the travel time and storage coefficient in an urban basin can be assumed to be identical.

4.2.2. *Evaluation of impulse response functions*

Fig. 7(a) and (b) compare the impulse response functions measured at the exit of each sub-basin, while Fig. 7(c) and (d) do the same, but are measured at the exit of the entire basin. Fig. 7(b) and (d) contain more graphs as the number of sub-basins are increased, as the building is additionally considered. As the building is introduced, a sub-basin is replaced by two: a rooftop sub-basin of the building, and another sub-basin representing the building wall. In fact, these two constitute the difference between the two cases of with and without the building. As a result of this difference, the resulting impulse response function (solid line in Fig. 7(d)) shows a slightly higher peak than that in Fig. 7(c) without the building. This is mainly due to the contribution from the building wall sub-basin. On the other hand, as the travel time significantly increases, the rooftop sub-basin, instead of the corresponding ground one, decreases the peak flow.

4.2.3. *Determination of experiment time*

The rainfall duration in the experiment was determined to confirm the occurrence of peak flow. Two different wind speeds of 0.80 and 1.11 m/s and three rainfall intensities were considered in this experiment with the building of width 0.8 m and height 1.4 m. Fig. 8 shows the observed runoff for 20 min in those experimental settings. Additionally, the same condition was applied for the rainfall–runoff simulation, whose result is also compared in the same figure:

This figure shows that the peak flow occurred at around 300 s in the experiment. On the other hand, the peak time in the rainfall–runoff simulation was found to be a bit retarded, compared with that of the experiment. This difference might be due to the rather long travel time on the building wall in the rainfall–runoff simulation. The simulation result shows that the peak flow occurred at about 800 s. Based on these experimental and simulation results, this study determined the rainfall duration to be 1,200 s. The runoff measurement was extended by an additional 600 s to see the behavior of the hydrograph in the falling limb. The simulation was also done for the same condition.

4.2.4. *Sensitivity analysis of the simulation results*

In this study, the authors conducted the sensitivity analysis of simulation results on peak value and travel time. The peak value of the shot noise is related to the peak flow of the hydrograph, and the travel

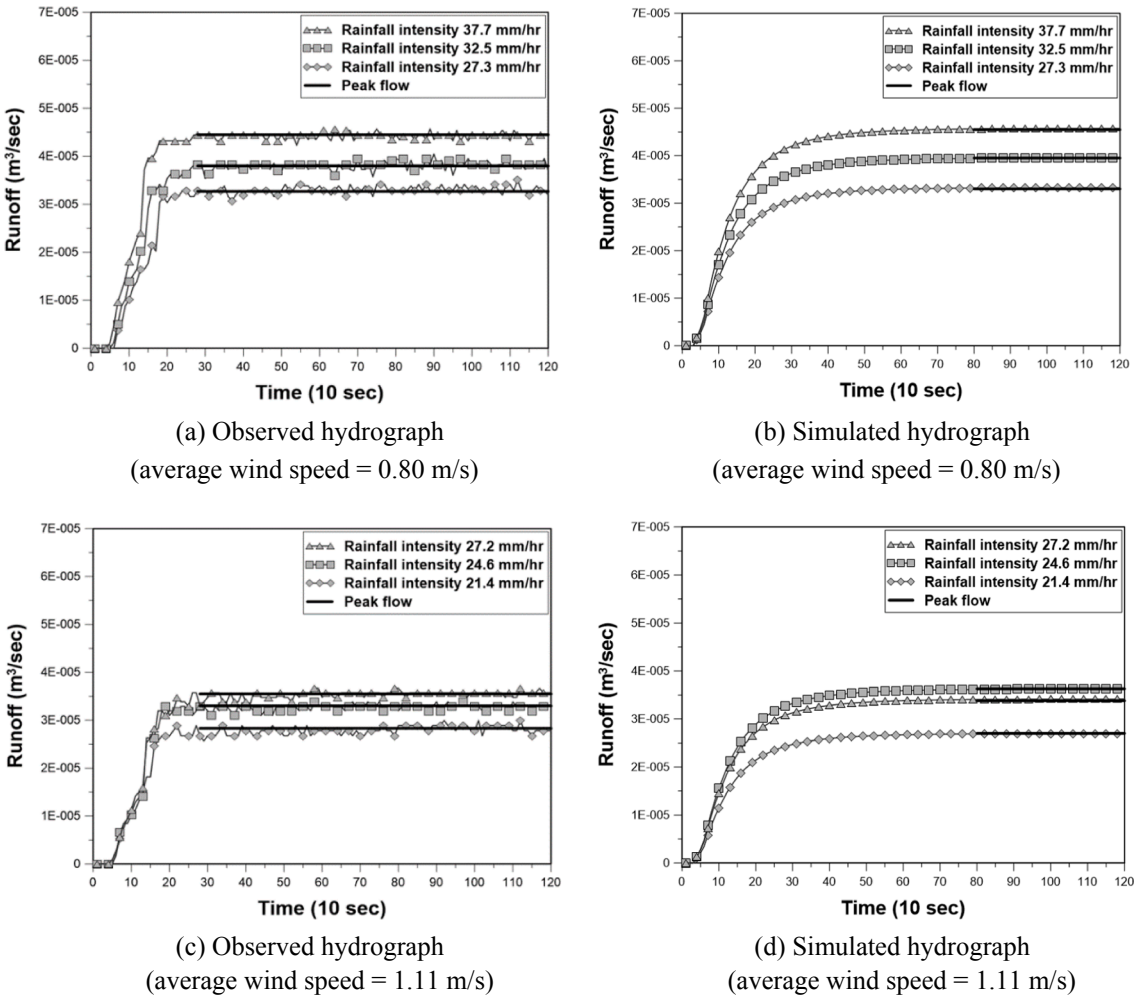

(a) Observed hydrograph (average wind speed = 0.80 m/s)

(b) Simulated hydrograph (average wind speed = 0.80 m/s)

(c) Observed hydrograph (average wind speed = 1.11 m/s)

(d) Simulated hydrograph (average wind speed = 1.11 m/s)

Fig. 8. Rainfall-runoff experiment for determination of experiment time.

time is related to the peak time and the recession curve. The peak value can be estimated by using the results of the modified rational formula, in which the key parameter is the runoff coefficient. In the experimental basin in this study, infiltration does not occur, and all rainfall contributes to the runoff. Therefore, the peak value was estimated assuming that the runoff coefficient of the basin is 1.0.

To analyze the sensitivity on the peak value, this study simulated the hydrograph by changing the runoff coefficients to 0.80, 0.85, 0.90, 0.95, and 1.00 while other parameters are fixed. To analyze the sensitivity on the travel time, the hydrograph was simulated by changing the average of the travel time to 50 sec, 70 sec, 90 sec, 110 sec, and 130 sec. In this analysis, the height of the building model was fixed to 1.4 m. Figs. 9-10 show the simulation results with various runoff coefficients and the average of the travel time.

Figs. 9-10 shows the influence of the peak value of the shot noise and travel time on the simulation results. In Fig. 9, as the runoff coefficient increases, the peak of the hydrograph also increases. When the runoff coefficient is 1.00, the peak flow is 1.25 times bigger than that with the runoff coefficient of 0.80. In Fig. 10, the peak time increases as the average of the travel time increases. When the average of the travel time was 130 sec, the peak time was increased by 2.32 times on average compared to that with the average of the travel time of 50 sec. Through the sensitivity analysis, the authors were able to confirm the effect of peak value and travel time on the simulation results in this study.

4.3. Comparison of the simulation and experimental results

In the rainfall–runoff simulation considering the building located at the center of the basin, it was required to add the WDR on the building wall. This study used the empirical equation by Cho et al. (2020) (i.e., Eq. (1) in Section 2), which is, in fact, the equation to estimate the amount of rainfall intercepted by a building. The amount of rainfall interception was then converted into the rainfall intensity over the building wall to be used as input of the rainfall–runoff model. For example, under the condition of the wind speed 1.62 m/s and rainfall intensity on the basin surface 27.2 mm/h, the rainfall amount intercepted by the building wall with its height 1.4 m and width 0.8 m comprises up to 27.4% of the rainfall amount collected over the rooftop of the building.

Fig. 11 compares the runoff results based on the experiment and simulation. All the symbols represent the experimental results, the circle represents the experimental results for the building height 1.4 m, the triangle for the building height 1.0 m, and the square with no building in the basin. The solid lines represent the simulation results, the darkest one for the building height 1.4 m, and the lightest one with no building in the basin.

Basically, the experimental results matched the simulation results well. The overall shape was the same, and the peak flows were also very similar to each other. However, in the simulation of the cases, the peak time was found to be slightly retarded, especially when considering the building at the center of the basin. This problem was also noticed in the pre-experiment for determining the rainfall duration for the experiment.

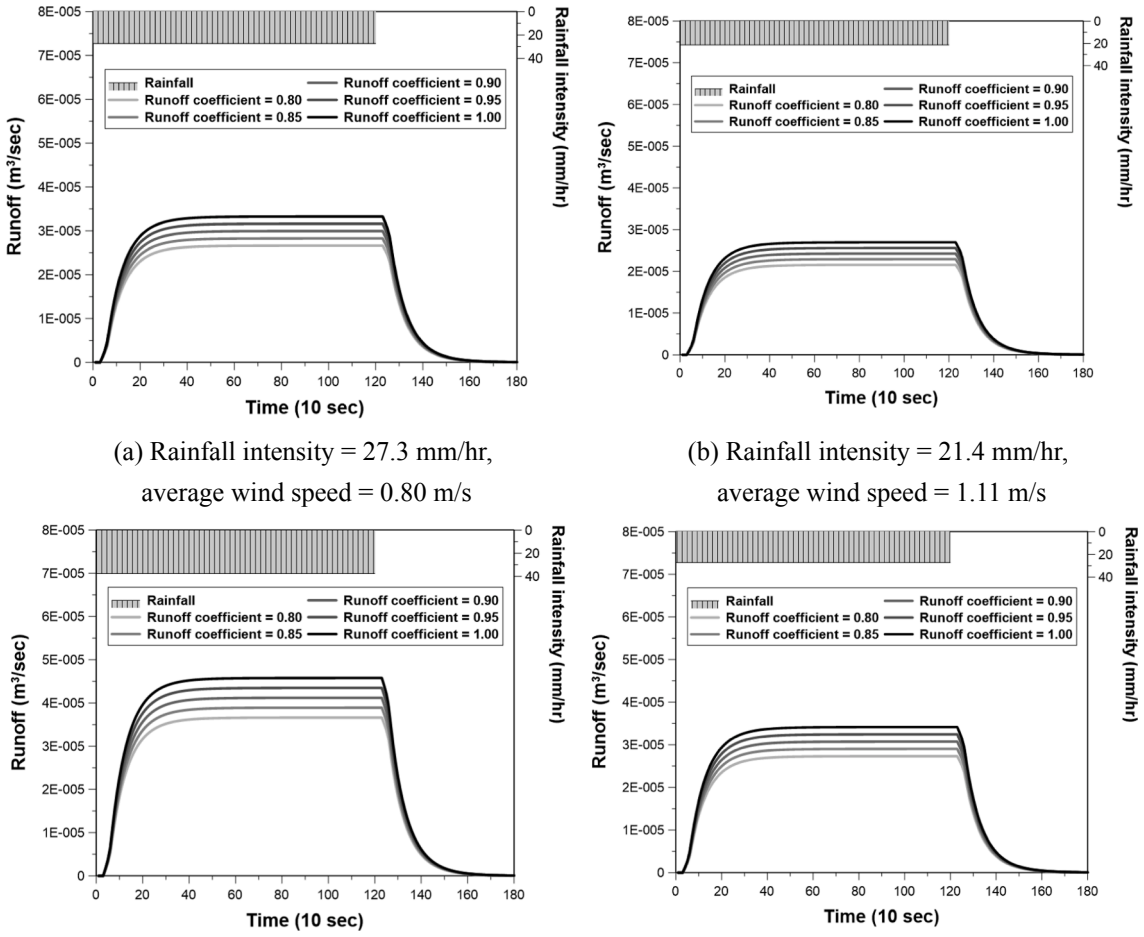

(a) Rainfall intensity = 27.3 mm/hr, average wind speed = 0.80 m/s

(b) Rainfall intensity = 21.4 mm/hr, average wind speed = 1.11 m/s

(c) Rainfall intensity = 37.7 mm/hr, average wind speed = 0.80 m/s

(d) Rainfall intensity = 27.2 mm/hr, average wind speed = 1.11 m/s

Fig. 9. Sensitivity analysis of peak value on simulated hydrograph.

This difference indicates a possible overestimation of the travel time in the building wall.

However, the difference between the cases with and without the building at the center of the basin was clearly evident. The difference between the cases with different building heights, even though it was smaller than that between the cases with and without the building, could also be clearly observed. As a result, the effect of the building wall on the runoff could be confirmed in this experiment. In particular, the contribution of the building wall to the peak flow was found to be highly significant, especially when the wind speed was high. For example, when the mean wind speed was 0.80 m/s, the contribution of the building wall on the peak flow was 2.9 – 3.9% for the building height 1.0 m, and 4.7 – 5.2% for the building height 1.4 m. It became even higher, when the mean wind speed was 1.11 m/s, to become 6.3 – 6.9% for the building height 1.0 m, and 14.2 – 17.0% for the building height 1.4 m.

If considering higher buildings, the contribution from the wall could be much higher than that from the rooftop of the building. Cho et al. (2020) estimated the amount of rainwater that could possibly be collected from the building wall according to the ratio of the wall area to the rooftop area. Based on their study, when the ratio of the wall area to the rooftop area is one, the rainwater collected from the building wall can be greater than 50% of the rainwater collected from the rooftop (under wind speed higher than 4 m/s). Furthermore, the amount of rainwater from the building wall can be greater than that from the rooftop if the ratio of the wall area to the rooftop area increases to 10, even in the case where the wind speed is only around 1 m/s.

In addition, the authors investigated how the RMSE and the difference between the peak flows changed in the case of considering the building. The observed hydrograph used in the analysis is the result of considering the building, and the simulated hydrographs are the results with and without considering the building. Table 5 shows the RMSE and Table 6 shows the difference between peak flows.

Table 5 shows that the accuracy of the rainfall-runoff model can be improved as the building is considered. In all cases, the RMSE between the observed and simulated hydrograph decreased as the building was considered. In some cases, the RMSE decreased by more than 50% as the building was considered. Table 6 also shows that the difference of peak flow decreases significantly as the building is considered.

5. Conclusions

This study proposed the rainfall–runoff analysis method considering the high-rise building in an urban basin. The high-rise building changes the role of rainfall interception and complicates the flow path of the runoff. The rooftop and wall of the building were assumed to be independent sub-basins to analyze the effect of high-rise buildings. The rainfall–runoff model based on the shot noise process was applied to consider the building rooftop sub-basin and the wall sub-basin independently. In addition, the rainfall–runoff experiment was conducted in a laboratory environment to validate the proposed method considering the high-rise buildings. The major results of this study can be

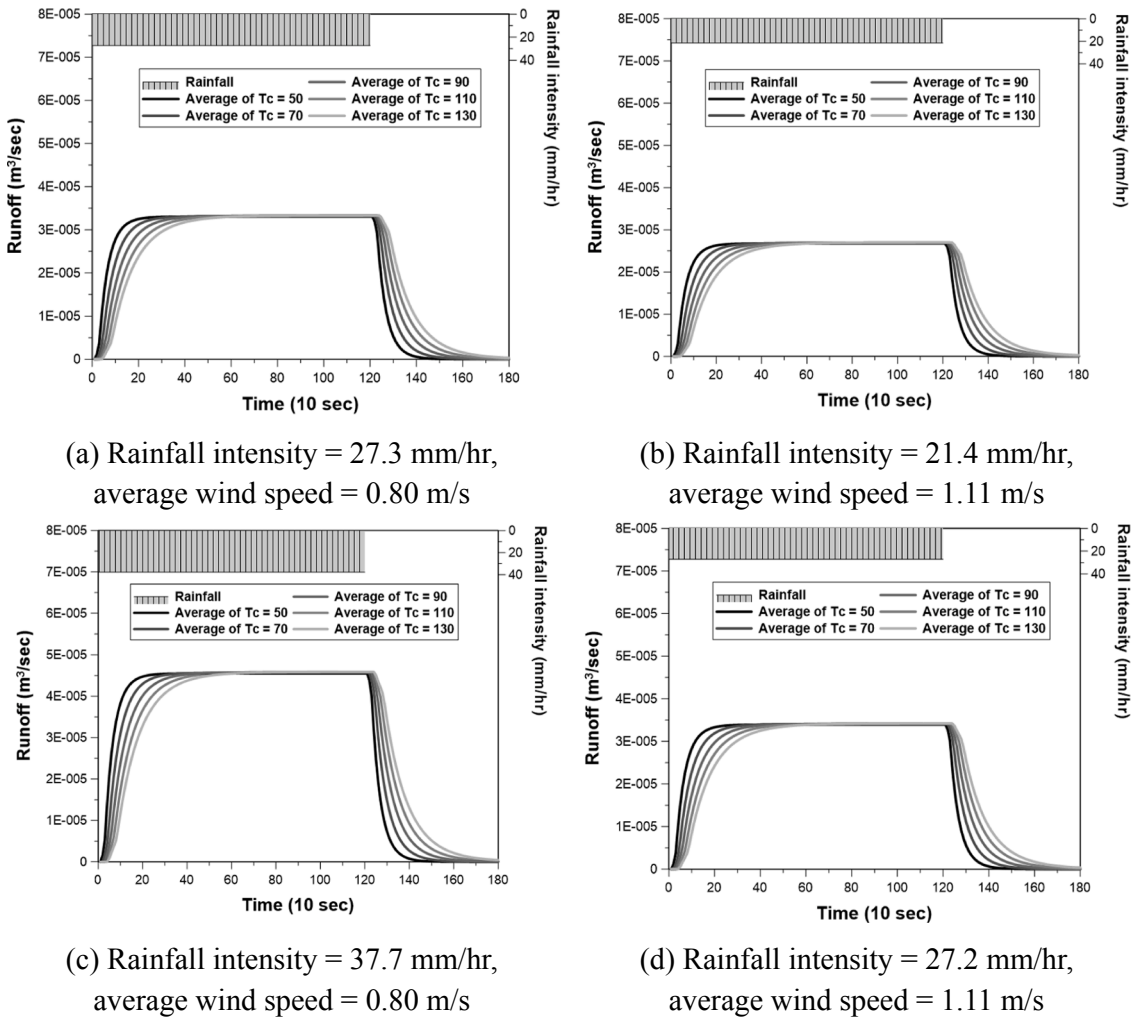

(a) Rainfall intensity = 27.3 mm/hr, average wind speed = 0.80 m/s

(b) Rainfall intensity = 21.4 mm/hr, average wind speed = 1.11 m/s

(c) Rainfall intensity = 37.7 mm/hr, average wind speed = 0.80 m/s

(d) Rainfall intensity = 27.2 mm/hr, average wind speed = 1.11 m/s

Fig. 10. Sensitivity analysis of travel time on simulated hydrograph.

summarized as follow:

(1) This study analyzed the effect of the high-rise building on the rainfall–runoff analysis. The intercepted rainfall by the building wall can contribute to the increase of the runoff volume and peak flow, but the longer flow path from the rooftop basin can decrease the peak flow. Overall, the role of the building wall was found to be more significant, resulting in increased runoff volume and peak flow.

(2) Both the simulation study and the experimental study were conducted to evaluate the effect of the high-rise building on the runoff. Both results, i.e., the runoff hydrographs, were very similar to each other, which confirms the effect of the high-rise building on the runoff. Additionally, the experimental result could validate the rainfall–runoff analysis method used in this study.

(3) It was confirmed that the contribution of the building wall to the peak flow was highly significant, particularly when the wind speed was high. For example, when the mean wind speed was 1.11 m/s, the contribution of the building wall to the peak flow was 6.3 – 6.9% for the building height 1.0 m, and 14.2 – 17.0% for the building height 1.4 m. If considering higher buildings, it becomes even higher. Based on Cho et al. (2020), if the ratio of the wall area to the rooftop area increases to 10, the amount of rainwater from the building wall can be larger than that from the rooftop, even in the case where the wind speed is only around 1 m/s.

(4) This study found that the accuracy of the rainfall-runoff model can be improved by considering the building. When the building was considered, the RMSE between the observed and simulated hydrograph decreased in all cases. In some cases, the RMSE decreased by more than 50%, and the difference of peak flow also decreased significantly as the building is considered.

The above results of this study confirm that in urban basins, the contribution of the high-rise building to the runoff can be significant. However, it should be mentioned that the experiment was conducted indoors, so it was impossible to satisfy all the conditions mimicking the natural phenomena. To conduct the more accurate experiment, the rainfall nozzle should be located very high for the raindrops to reach the terminal velocity. However, the maximum height available in the lab was just 3.0 m. That is, the rainfall simulation may be assumed to be somewhat limited. Instead, Cho et al. (2020) tried to prove the applicability of the empirical equation using the data collected from a building model located on the rooftop of Engineering Hall, Korea University located in Seoul, Korea. Fortunately, the result was very similar to that derived in the lab, and, as a result, the authors could confirm that the empirical equation derived is valid.

In addition, this study simulated the rainfall-runoff processes using various empirical formulas. In this study, the empirical formulas worked well in the laboratory scale, but it is true that the authors cannot guarantee their applicability to the real world. To prove the applicability of those empirical equations, it is necessary to analyze the observed data collected from the real basin. The authors are currently conducting additional research to verify the methodology proposed in this study. The authors also expect that the proposed empirical formula can be applied to real world with real buildings and real urban basins.

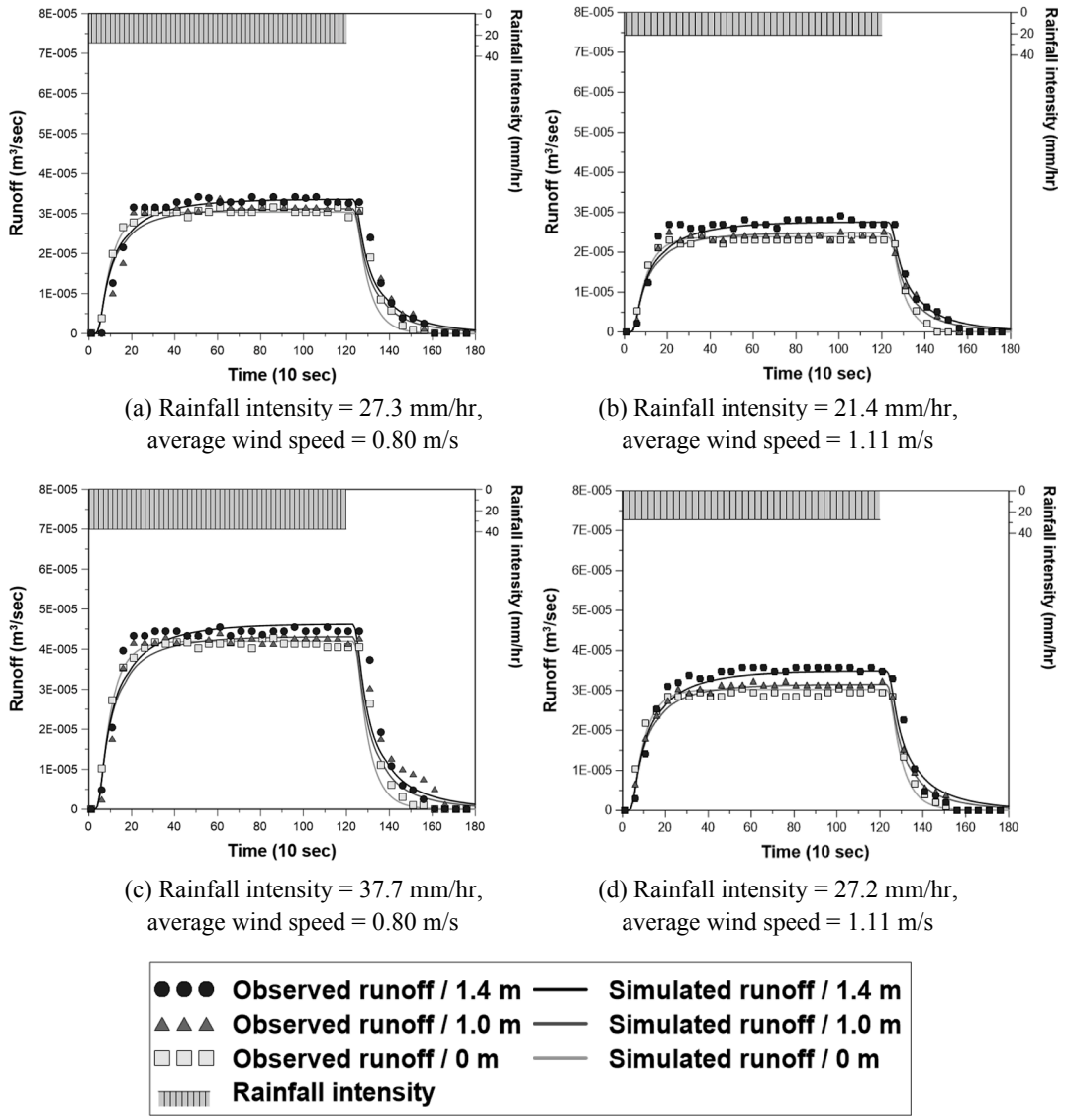

(a) Rainfall intensity = 27.3 mm/hr, average wind speed = 0.80 m/s

(b) Rainfall intensity = 21.4 mm/hr, average wind speed = 1.11 m/s

(c) Rainfall intensity = 37.7 mm/hr, average wind speed = 0.80 m/s

(d) Rainfall intensity = 27.2 mm/hr, average wind speed = 1.11 m/s

Fig. 11. Comparison of observed and simulated hydrograph in experimental basin.

Table 5
RMSEs ($10^{-6}m^3$/sec) with and without considering building.

Wind speed (m/s)	Rainfall intensity (mm/hr)	Without considering building Building height (m)		With considering building Building height (m)	
		1.0	1.4	1.0	1.4
0.80	27.3	3.93	2.79	3.28	2.18
	37.7	4.34	5.23	3.49	3.50
1.11	21.4	1.55	2.74	1.27	1.28
	27.2	1.76	4.16	1.22	1.79

Table 6
Difference of peak flow ($10^{-6}m^3$/sec) with and without considering building.

Wind speed (m/s)	Rainfall intensity (mm/hr)	Without considering building Building height (m)		With considering building Building height (m)	
		1.0	1.4	1.0	1.4
0.80	27.3	4.00	2.90	3.50	0.30
	37.7	3.30	4.10	2.70	0.11
1.11	21.4	1.60	4.30	1.00	0.90
	27.2	2.30	5.60	1.50	1.50

CRediT authorship contribution statement

Chulsang Yoo: Conceptualization, Supervision, Writing - review & editing. **Eunsaem Cho:** Visualization, Investigation, Data curation, Formal analysis, Writing - original draft. **Wooyoung Na:** Methodology, Software. **Minseok Kang:** Data curation. **Munseok Lee:** .

Declaration of Competing Interest

The authors declare that they have no known competing financial interests or personal relationships that could have appeared to influence the work reported in this paper.

Acknowledgments

This work is supported by a grant (19CTAP-C143641-02) from

Infrastructure and Transportation Technology Promotion Research Program funded by Ministry of Land Infrastructure and Transport of Korean government and the National Research Foundation of Korea grant funded by the Korea government (2020R1A2C2008714).

References

Bedient, P.B., Huber, W.C., Vieux, B.E., 2008. Hydrology and floodplain analysis. Pearson Education, London, England.

Beijer, O., Johansson, A., 1977. Driving rain against external walls of concrete. Swedish Cement and Concrete Research Institute at the Institute of Technology, Stockholm, Sweden.

Bicknell, B.R., Imhoff, J.C., Kittle Jr, J.L., Donigian Jr, A.S., Johanson, R.C., 1996. Hydrological simulation program-FORTRAN. user's manual for release 11. United States Environmental Protection Agency, Washington, D.C., USA.

Bisht, D.S., et al., 2016. Modeling urban floods and drainage using SWMM and MIKE URBAN: a case study. Nat. Hazards 84 (2), 749–776.

Blocken, B., Carmeliet, J., 2012. A simplified numerical model for rainwater runoff on building facades: Possibilities and limitations. Build. Environ. 53, 59–73.

Cançado, V., Brasil, L., Nascimento, N., Guerra, A., 2008. Flood risk assessment in an urban area: Measuring hazard and vulnerability, 11th International conference on urban drainage. Edinburgh, Scotland, pp. 1–10.

Cea, L., Garrido, M., Puertas, J., 2010. Experimental validation of two-dimensional depth-averaged models for forecasting rainfall–runoff from precipitation data in urban areas. J. Hydrol. 382 (1–4), 88–102.

Chan, Y., 2012. Rainfall-runoff processes in urban environments. University of Cambridge, U.K.

Chen, Y., Zhou, H., Zhang, H., Du, G., Zhou, J., 2015. Urban flood risk warning under rapid urbanization. Environ. Res. 139, 3–10.

Cho, E., Yoo, C., Kang, M., Song, S., Kim, S., 2020. Experiment of Wind-Driven-Rain Measurement on Building Walls and Its In-situ Validation. Environ, Build in press.

Clark, C., 1945. Storage and the unit hydrograph. Proc. Am. Soc. Civ. Eng. 69 (9), 1333–1360.

Cleophas, C., Cottrill, C., Ehmke, J.F., Tierney, K., 2019. Collaborative urban transportation: recent advances in theory and practice. Eur. J. Oper. Res. 273 (3), 801–816.

Cole, G., Shutt, J., 1976. SWMM as a predictive model for runoff, Proceedings of the National Symposium on Urban Hydrology, Hydraulics, and Sediment Control, Kenturcky, USA, pp. 193-201.

De Vogelaere, T., Pacco, M., 2012. Development of a numerical model for rainwater run-off on vertical planes extended with experimental verification. Master thesis Thesis. Ghent University, Ghent, Belgium.

DESA, U., 2018. World Urbanization Prospects: The 2018 Revision. Key Facts, United Nations Department of Economic and Social Affairs, New York, USA.

Diskin, M., Buras, N., Zamir, S., 1973. Application of a simple hydrologic model for rainfall-runoff relations of the Dalton Watershed. Water Resour. Res. 9 (4), 927–936.

Dottori, F., Todini, E., 2013. Testing a simple 2D hydraulic model in an urban flood experiment. Hydrol. Processes 27 (9), 1301–1320.

Douglas, I., 2012. Urban ecology and urban ecosystems: understanding the links to human health and well-being. Curr. Opin. Environ. Sust. 4 (4), 385–392.

Du, J., et al., 2012. Assessing the effects of urbanization on annual runoff and flood events using an integrated hydrological modeling system for Qinhuai River basin. China. J. Hydrol. 464, 127–139.

Ferreira, C., et al., 2019. Impacts of distinct spatial arrangements of impervious surfaces on runoff and sediment fluxes from laboratory experiments. Anthropocene 28, 100219.

Ferro, V., 2001. Tecniche di misura e monitoraggio dei processi erosivi. Quad. Idron. Mont. 21 (2), 63–128.

Gabel, J., Shehadi, A., 2017. CTBUH year in review: tall trends of 2016: 2016 another record-breaker for skyscraper completions; 18 "Tallest Titles" Bestowed. CTBUH J. 1, 38–45.

Grimmond, C.S.B., Oke, T.R., 1991. An evapotranspiration-interception model for urban areas. Water Resour. Res. 27 (7), 1739–1755.

Hall, C., Kalimeris, A., 1982. Water movement in porous building materials—V. Absorption and shedding of rain by building surfaces. Build. Environ. 17 (4), 257–262.

Hamdi, R., Termonia, P., Baguis, P., 2011. Effects of urbanization and climate change on surface runoff of the Brussels Capital Region: a case study using an urban soil–vegetation–atmosphere-transfer model. Int. J. Climatol. 31 (13), 1959–1974.

Hejazi, M.I., Markus, M., 2009. Impacts of urbanization and climate variability on floods in Northeastern Illinois. J. Hydrol. Eng. 14 (6), 606–616.

Hua, J., Liang, Z., Yu, Z., 2003. A modified rational formula for flood design in small basins 1. J. Am. Water Resour. Assoc. 39 (5), 1017–1025.

Huang, M., Jin, S., 2019. A methodology for simple 2-D inundation analysis in urban area using SWMM and GIS. Nat. Hazards 97 (1), 15–43.

Hughes, M., Hall, A., Fovell, R.G., 2009. Blocking in areas of complex topography, and its influence on rainfall distribution. J. Atmos. Sci. 66 (2), 508–518.

Isidoro, J., De Lima, J., 2014. Laboratory simulation of the influence of building height and storm movement on the rainfall run-off process in impervious areas. J. Flood Risk Manage. 7 (2), 176–181.

Isidoro, J.M., de Lima, J.L., Leandro, J., 2012. Influence of wind-driven rain on the rainfall-runoff process for urban areas: scale model of high-rise buildings. Urban Water J. 9 (3), 199–210.

JSCE, 1999. The Collection of Hydraulic Formulae. Japan Society of Civil Engineers, Tokyo, Japan.

Jung, C.G., Kim, S.J., 2017. Evaluation of land use change and groundwater use impact on stream drying phenomena using a grid-based continuous hydrologic model. Paddy Water Environ. 15 (1), 111–122.

Kang, M., Yoo, C., 2018. Development of a shot noise process based rainfall-runoff model for urban flood warning system. J. Korea Water Resour. Assoc. 51 (1), 19–33.

Kerby, W., 1959. Time of concentration for overland flow. Civ. Eng. 29, 60.

Kirpich, Z., 1940. Time of concentration of small agricultural watersheds. Civ. Eng. 10 (6), 362.

Leandro, J., Martins, R., 2016. A methodology for linking 2D overland flow models with the sewer network model SWMM 5.1 based on dynamic link libraries. Water Sci. Technol. 73 (12), 3017–3026.

Leandro, J., Schumann, A., Pfister, A., 2016. A step towards considering the spatial heterogeneity of urban key features in urban hydrology flood modelling. J. Hydrol. 535, 356–365.

Lemonsu, A., Masson, V., Berthier, E., 2007. Improvement of the hydrological component of an urban soil–vegetation–atmosphere–transfer model. Hydrol. Processes 21 (16), 2100–2111.

Li, G.-F., Xiang, X.-Y., Tong, Y.-Y., Wang, H.-M., 2013. Impact assessment of urbanization on flood risk in the Yangtze River Delta. Stoch. Environ. Res. Risk Asssess. 27 (7), 1683–1693.

Linsley, R., 1945. Discussion of storage and the unit hydrograph by CO Clark. Trans. Am. Soc. Civ. Eng. 110, 1452–1455.

Liu, W., Feng, Q., Deo, R.C., Yao, L., Wei, W., 2020. Experimental study on the rainfall-runoff responses of typical urban surfaces and two green infrastructures using scale-based models. Environ. Manage. 66 (4), 683–693.

Liu, X., et al., 2018. High-resolution multi-temporal mapping of global urban land using Landsat images based on the Google Earth Engine Platform. Remote Sens. Environ. 209, 227–239.

Liu, Y., De Smedt, F., Hoffmann, L., Pfister, L., 2005. Assessing land use impacts on flood processes in complex terrain by using GIS and modeling approach. Environ. Model. Assess. 9 (4), 227–235.

Maidment, D.R., 1993. Handbook of hydrology. McGraw-Hill New York, New York, USA.

ME, 2015. Guidelines for establishing the basic plan for sewerage maintenance. Sejong, Korea.

Murphy, S.F., Stallard, R.F., Scholl, M.A., González, G., Torres-Sánchez, A.J., 2017. Reassessing rainfall in the Luquillo Mountains, Puerto Rico: Local and global ecohydrological implications. PloS one 12 (7), e0180987.

Nash, J.E., HRS, 1960. A unit hydrograph study, with particular reference to British catchments. Proc. Inst. Civ. Eng. 17 (3), 249–282.

Niemi, T.J., Kokkonen, T., Sillanpää, N., Setälä, H., Koivusalo, H., 2019. Automated urban rainfall-runoff model generation with detailed land cover and flow routing. J. Hydrol. Eng. 24 (5), 04019011.

Nirupama, N., Simonovic, S.P., 2007. Increase of flood risk due to urbanisation: a Canadian example. Nat. Hazards 40 (1), 25.

O'Driscoll, M., Clinton, S., Jefferson, A., Manda, A., McMillan, S., 2010. Urbanization effects on watershed hydrology and in-stream processes in the southern United States. Water 2 (3), 605–648.

Pappas, E., Smith, D., Huang, C., Shuster, W., Bonta, J., 2008. Impervious surface impacts to runoff and sediment discharge under laboratory rainfall simulation. Catena 72 (1), 146–152.

Phillis, Y.A., Kouikoglou, V.S., Verdugo, C., 2017. Urban sustainability assessment and ranking of cities. Comput. Environ. Urban Syst. 64, 254–265.

Ponce, V.M., 1989. Engineering hydrology: Principles and practices. Englewood Cliffs, New Jersey, USA.

Prosdocimi, I., Kjeldsen, T., Miller, J., 2015. Detection and attribution of urbanization effect on flood extremes using nonstationary flood-frequency models. Water Resour. Res. 51 (6), 4244–4262.

Roy, A.H., Dybas, A.L., Fritz, K.M., Lubbers, H.R., 2009. Urbanization affects the extent and hydrologic permanence of headwater streams in a midwestern US metropolitan area. J. N. Am. Benthol. Soc. 28 (4), 911–928.

Russell, S.O., Sunnell, G.J., Kenning, B.F., 1979. Estimating design flows for urban drainage. J. Hydraul. Div. 105 (1), 43–52.

Rziha, F., 1876. Eisenbahn-Unter-und Oberbau. Verlag der KK Hof-und Staatsdruckerei, Vienna, Austria.

Sabol, G.V., 1988. Clark unit hydrograph and R-parameter estimation. J. Hydraul. Eng. 114 (1), 103–111.

Safarik, D., Wood, A., Carver, M., Gerometta, M., 2015. A year in review: tall trends of 2014: an all-time record 97 buildings of 200 meters or higher completed in 2014. CTBUH J. 1, 40–47.

Saghafian, B., Farazjoo, H., Bozorgy, B., Yazdandoost, F., 2008. Flood intensification due to changes in land use. Water Resour. Manag. 22 (8), 1051–1067.

Sahoo, B., Chatterjee, C., Raghuwanshi, N.S., Singh, R., Kumar, R., 2006. Flood estimation by GIUH-based Clark and Nash models. J. Hydrol. Eng. 11 (6), 515–525.

Schubert, J.E., Sanders, B.F., Smith, M.J., Wright, N.G., 2008. Unstructured mesh generation and landcover-based resistance for hydrodynamic modeling of urban flooding. Adv. Water Resour. 31 (12), 1603–1621.

Seto, K.C., Shepherd, J.M., 2009. Global urban land-use trends and climate impacts. Curr. Opin. Environ. Sust. 1 (1), 89–95.

Seyoum, S.D., Vojinovic, Z., Price, R.K., Weesakul, S., 2012. Coupled 1D and noninertia 2D flood inundation model for simulation of urban flooding. J. Hydraul. Eng. 138 (1), 23–34.

Shuster, W., Pappas, E., 2011. Laboratory simulation of urban runoff and estimation of runoff hydrographs with experimental curve numbers implemented in USEPA SWMM. J. Irrig. Drain. Eng. 137 (6), 343–351.

Shuster, W., Pappas, E., Zhang, Y., 2008. Laboratory-scale simulation of runoff response from pervious-impervious systems. J. Hydrol. Eng. 13 (9), 886–893.
Singh, S.K., 2004. Simplified use of gamma-distribution/Nash model for runoff modeling. J. Hydrol. Eng. 9 (3), 240–243.
Soliman, M.M., 2010. Engineering hydrology of arid and semi-arid regions. CRC Press, Florida, USA.
Suriya, S., Mudgal, B., 2012. Impact of urbanization on flooding: the Thirusoolam sub watershed–a case study. J. Hydrol. 412, 210–219.
Terstriep, M.L., Stall, J.B., 1974. The Illinois urban drainage area simulator. ILLUDAS, Illinois, USA.
Tingsanchali, T., 2012. Urban flood disaster management. Procedia Eng. 32, 25–37.
USDA, 1985. National engineering handbook, section 4: hydrology. United States Department of Agriculture, Washington, D.C., USA.
Weiss, G., 1977. Shot noise models for the generation of synthetic streamflow data. Water Resour. Res. 13 (1), 101–108.
Wiles, J.J., Levine, N.S., 2002. A combined GIS and HEC model for the analysis of the effect of urbanization on flooding; the Swan Creek watershed. Ohio. Environ. Eng. Geosci. 8 (1), 47–61.
Wyly, R.S., Eaton, H.N., 1961. Capacities of stacks in sanitary drainage systems for buildings, 31. US Department of Commerce, National Bureau of Standards, Maryland, USA.
Yao, L., Wei, W., Chen, L., 2016. How does imperviousness impact the urban rainfall-runoff process under various storm cases? Ecol. Indic. 60, 893–905.
Zhou, D., Zhao, S., Zhang, L., Sun, G., Liu, Y., 2015. The footprint of urban heat island effect in China. Sci. Rep. 5 (1), 1–11.